Impact of heat pump load on distribution networks

AKMAL, M. <http://orcid.org/0000-0002-3498-4146>, FOX, B., MORROW, J.D. and LITTLER, T.

Published version

AKMAL, M., FOX, B., MORROW, J.D. and LITTLER, T. (2014). Impact of heat pump load on distribution networks. IET Generation, Transmission and Distribution, 8 (12), 2065-2073.

Published in IET Generation, Transmission & Distribution
Received on 23rd January 2014
Revised on 9th May 2014
Accepted on 21st May 2014
doi: 10.1049/iet-gtd.2014.0056

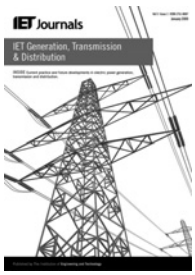

ISSN 1751-8687

Impact of heat pump load on distribution networks

Muhammad Akmal[1], *Brendan Fox*[2], *John David Morrow*[2], *Tim Littler*[2]

[1]*College of Engineering, Abu Dhabi University, Abu Dhabi, UAE*
[2]*Energy, Power and Intelligent Control, Queen's University Belfast, Belfast BT9 5AH, UK*
E-mail: makmal01@qub.ac.uk

Abstract: Heat pumps can provide domestic heating at a cost that is competitive with oil heating in particular. If the electricity supply contains a significant amount of renewable generation, a move from fossil fuel heating to heat pumps can reduce greenhouse gas emissions. The inherent thermal storage of heat pump installations can also provide the electricity supplier with valuable flexibility. The increase in heat pump installations in the UK and Europe in the last few years poses a challenge for low-voltage networks, because of the use of induction motors to drive the pump compressors. The induction motor load tends to depress voltage, especially on starting. The study includes experimental results, dynamic load modelling, comparison of experimental results and simulation results for various levels of heat pump deployment. The simulations are based on a generic test network designed to capture the main characteristics of UK distribution system practice. The simulations employ DIgSlILENT Power Factory to facilitate dynamic simulations that focus on starting current, voltage variations, active power, reactive power and switching transients.

1 Introduction

The UK and Ireland have a cool maritime climate, with a heating season of about 7 months. Daily average temperature rarely falls below freezing point. These conditions are ideal for the effective operation of heat pumps, whose efficiency is inversely proportional to the temperature difference between the heated space and the environment. The inexorable rise in oil and gas prices has encouraged the adoption of heat pumps. Ground-source heat pumps are typically installed in new, detached dwellings whereas air source is generally more suited for retrofit applications [1]. The coefficient of performance, which is the heat produced per unit of electrical energy consumed, is typically in the range 3.0–4.0. If the supply generation is predominantly fossil fuel, with a thermal efficiency of about 35%, the heat produced by the heat pump is little more than what could be obtained directly from the fossil fuel. However, if a significant proportion of the generation is nuclear and/or renewable, then the heat pump can help to reduce overall fossil-fuel usage. Nuclear generation is responsible for about 20% of generation in Britain, while renewable, mainly wind generation supplies a similar proportion of demand in Ireland. Hence heat pumps can reduce fossil-fuel usage across the region, and the growing penetration of renewable generation will lead to further reduction. Often the choice is between an oil-fired central heating boiler with an efficiency of about 70% and a heat pump with under-floor heating. The economic and climate change arguments are now converging, with the result that heat pumps are likely to become more popular for new, detached dwellings [2].

A significant heat pump load brings a number of benefits to power system operators. In particular, the thermal inertia of modern dwellings is such that the pump can be switched off for several hours with minimal effect on temperature [3]. There are tariffs that deliver cheaper electricity for 21 h each day, counter-balanced by much more expensive electricity in the peak period, typically 4–7 p.m. This improves generation load factor, and also offers the following possibilities:

- use as emergency reserve – provided there is rapid communication and a tariff incentive;
- heat pump motor inertia helps to stabilise the system at times of significant renewable generation.

However, the growth of heat pump load poses a challenge for distribution engineers. A typical 10 kW heat pump will have a 2.5 kW compressor motor. Even with a soft-starter, the starting current will be around twice the normal running current. In addition to switching transients, the new induction motor load will tend to depress feeder voltage, especially if several such loads are connected to the feeder [4]. There may even be the possibility of voltage collapse.

The authors have assessed the potential problems by considering the static and dynamic effects of varying heat pump deployments on a generic distribution network [5, 6]. The work utilises the DIgSILENT power system simulation package. Modelling the heat pump compressor motor was a particular challenge, as standard simulation packages do not include models for the single-phase induction motors required for domestic heat pumps [7, 8]. Also, starting transients will depend on the dynamics of the compressor itself. It was considered that the most reliable approach was to monitor an actual heat pump motor, and to develop a model that could be integrated with DIgSILENT. It was

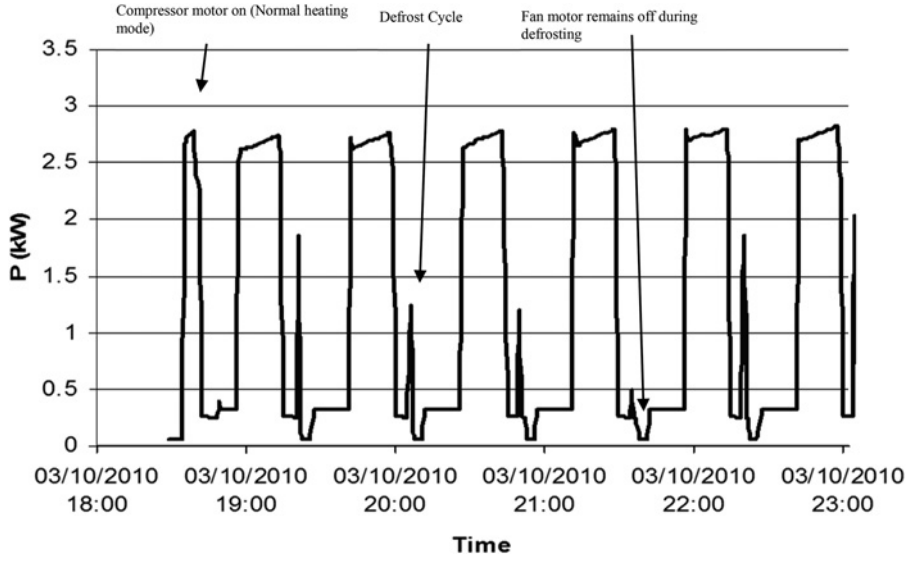

Fig. 1 *Electric power consumed by heat pump during operation cycles*

then possible to examine switching transients for various scenarios, including unbalanced loading.

2 Heat pump testing

Tests were conducted on a 10 kW air-source heat pump which had been fitted to the University laboratory. The refrigerant is evaporated by the ambient air, thus absorbing its latent heat of evaporation. The compressor compresses the vapour, which liquefies and returns the latent heat to a tank of water surrounding the refrigerant. The water provides under-floor heating to a university laboratory. It should be noted that the electrical behaviour of the compressor motor, which is the main interest here, is similar for both air-source and ground-source heat pumps.

Fig. 1 shows the power consumed by the heat pump over a 4.5 h period. The main feature is a duty cycle for the compressor motor, which will depend on the energy required to achieve a given temperature in the laboratory. The minor features of the graph show the operation of the fan motor, the reversing valve and the circulating pumps.

Fig. 2 shows the compressor motor instantaneous starting current.

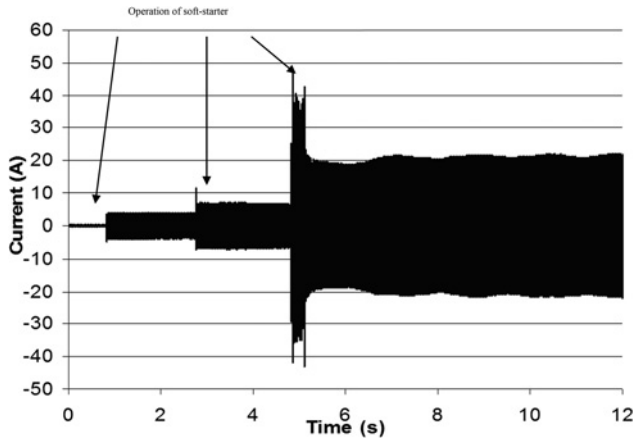

Fig. 2 *Real-time starting current of heat pump*

The starting current was found to peak at 28 A (r.m.s.), double the normal running current of 14 A (r.m.s.). Induction motor starting current is typically 4–7 times full-load current [9]. The reduced starting current is due to the use of a soft-starter, which results in the stepped increase in current seen in Fig. 2. As the compressor motor accounts for 90% of the heat pump load, these motor starts will dominate the impact of heat pumps on the distribution network. Hence, it was decided to develop a detailed model of this aspect of heat pump load.

3 Load modelling

The electricity supply to domestic consumers is single phase; hence, domestic heat pumps use single-phase induction motors to drive the compressor. This created a difficulty, as none of the major power system simulation packages, including DIgSILENT, provide a single-phase induction motor model. Single-phase induction motor models are presented in [7, 8], but without a soft-starter. It was therefore decided to create a model for use with DIgSILENT using the dynamic simulation language DSL.

The variations of heat pump active and reactive powers in response to terminal voltage and frequency are modelled to reproduce the experimental values as closely as possible. Models with and without a soft-starter were developed. First of all, general load modelling equations have been used. Active power is given by

$$P = P_0\left(k_{P1} \times \left(\frac{v}{V_0}\right)^{e_{P1}} + k_{P2} \times \left(\frac{v}{V_0}\right)^{e_{P2}} + \left(1 - k_{P1} - k_{P2}\right) \times \left(\frac{v}{V_0}\right)^{e_{P3}}\right) \quad (1)$$

Similarly for reactive power

$$Q = Q_0\left(k_{Q1} \times \left(\frac{v}{V_0}\right)^{e_{Q1}} + k_{Q2} \times \left(\frac{v}{V_0}\right)^{e_{Q2}} + \left(1 - k_{Q1} - k_{Q2}\right) \times \left(\frac{v}{V_0}\right)^{e_{Q3}}\right) \quad (2)$$

doi: 10.1049/iet-gtd.2014.0056

Table 1 Initial conditions and values of constants

Constant	Value	Constant	Value	Constant	Value
P_0	3 kW	k_{P1}	1	e_{P1} and e_{Q1}	1
Q_0	1.5 kVAR	k_{Q1}	1	e_{P2} and e_{Q2}	0
V_0	230 V	k_{P2}	0	e_{P3} and e_{Q3}	0
T	0.5 s	k_{Q2}	0	k_f	0.75

P_0, Q_0 and V_0 are the ratings of the load under consideration and are used as initial conditions for the respective time-dependent variable. P and Q are active and reactive powers, respectively. v is the time-dependent terminal voltage. The coefficients (k_{P1}, k_{P2}, k_{Q1} and k_{Q2}) determine the dependency of P and Q on the change in voltage, whereas the exponents (e_{P1}, e_{P2}, e_{P3}, e_{Q1}, e_{Q2} and e_{Q3}) specify the order of dependence on voltage. For a linear model, both k_{P1} and e_{P1} are unity and all remaining coefficients and exponents are zero in (1). Similarly, k_{Q1} and e_{Q1} are unity in (2). Standard parameter values for specific loads are used and it is found that the performance deviates considerably. This may be due to the inclusion of the soft-starter. For this reason, the experimental values are used to derive the model.

After considering linear dependency on voltage variations, a load time constant has been used which represents how long the load takes to follow the variations in the voltage. Assuming x_p as a state variable for dynamic calculation of active power, x_q for reactive power and T as the time constant

$$\frac{dx_p}{dt} = \frac{P - x_p}{T} \tag{3}$$

Similarly

$$\frac{dx_q}{dt} = \frac{Q - x_q}{T} \tag{4}$$

According to the experimental results, the compressor motor starts in three distinct stages.

(i) The first stage starts at the time when the switch has been closed. For this time the compressor motor draws power equivalent to $P_0/5$ for 2 s.
(ii) The second stage also lasts 2 s but this time the power drawn is $P_0/3$.
(iii) The third stage involves higher starting current for about 0.5 s. This stage has been modelled using a difference of two exponentials with different exponents to obtain the peak value of the experimental readings. Time delays are introduced to reproduce the exact shape of the experimental peak power.

The staged start is due to the soft-starter and the objective was to reproduce the shape mathematically for use in the DIgSILENT simulation. If t_s is the switching instant of the heap pump load, the equation will be (see (5)).

Similar equations are used for dynamic calculation of Q.

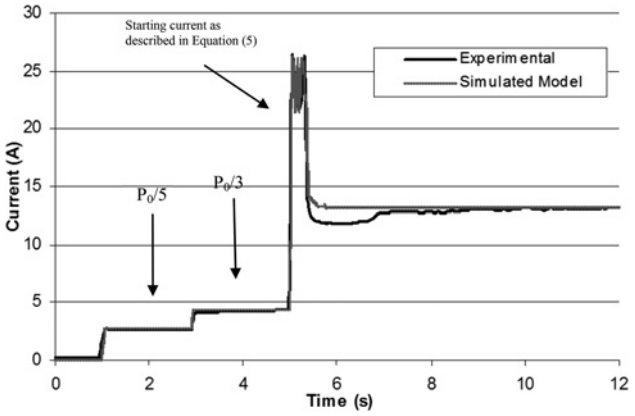

Fig. 3 *Comparison of experimental and simulation models for heat pump*

Frequency has been compared with the reference (50 Hz) and the difference has been used with a load-frequency constant to calculate the change in active power

$$\Delta P = k_f \times \Delta f \tag{6}$$

k_f is the load-frequency constant for the compressor motor. The values used in the model are given in Table 1.

This model has been validated against the experimental results. The r.m.s. values of current drawn by the experimental and simulated model are compared in Fig. 3. The load has been switched on at 1 s.

4 Test network

The UK generic distribution network (UKGDN) is shown in Fig. 4. It includes a 33/11.5 kV substation that supplies six 11 kV feeders. Each feeder serves 3072 customers, evenly distributed between eight 11/0.433 kV, 500 kVA transformers and an equal number of 400 V substations.

Each 400 V substation serves 384 single-phase consumers through four radial feeders, each with 96 consumers in four clusters of 24, 8 per phase. One feeder is modelled in detail and the rest are treated as lumped loads. The network was assessed by a number of distribution network operators and considered as representative of urban/suburban UK distribution networks. The most remote consumer is 3.33 km from the 33/11.5 kV substation. The full network data may be found in [5, 6].

The network, shown in Fig. 4, was modelled in DIgSILENT. The loads comprise: (i) the normal consumer demand of 1.3 kVA with power factor 0.95 lagging; and (ii) an optional heat pump described by the model in the previous section. The normal load is assumed to have a coincidence factor of 0.7.

5 Results

The steady-state and transient effects of heat pump load have been assessed by considering an increasing penetration of

$$P = \begin{cases} 0, & \text{if } t \le t_s \\ P_0/5, & \text{if } t_s < t \le t_s + 2 \\ P_0/3, & \text{if } t_s + 2 < t \le t_s + 4 \\ x_p \times \left(1 + 3 \times e^{(-1\times(t-t_s-4)/T)}\right) - 3 \times e^{(-2.7\times(t-t_s-4)/T)}, & \text{if } t > t_s + 4 \end{cases} \tag{5}$$

doi: 10.1049/iet-gtd.2014.0056

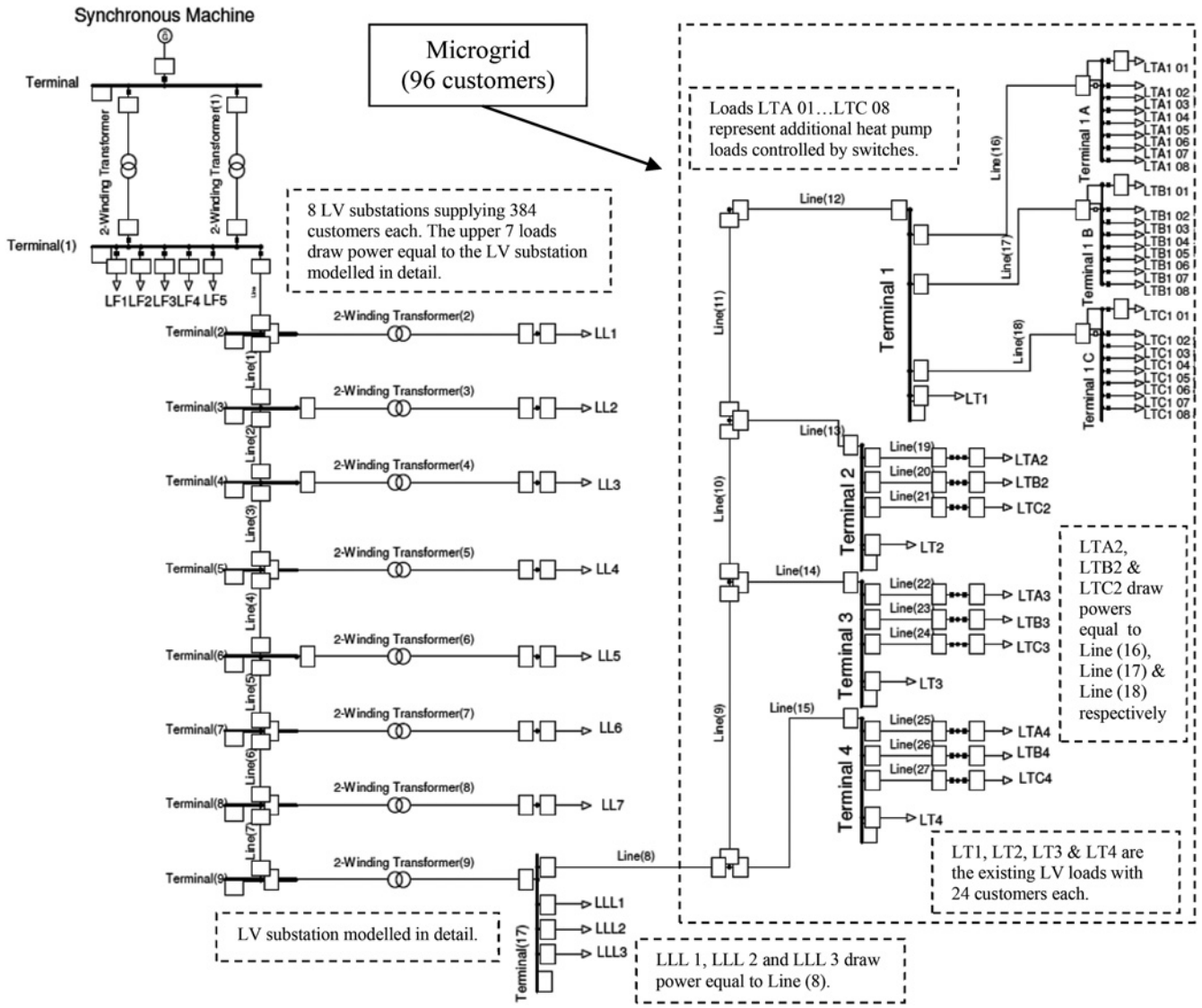

Fig. 4 *Test network modelled in DIgSILENT*

heat pumps in each cluster of 24 consumers on a single 400 V feeder [10].

5.1 Steady-state effect of increasing penetration

Penetration is 100% if all the consumers have a heat pump. If all 24 heat pumps in a cluster are switched on, then the lumped loads across the entire UKGDN are set to reflect the same penetration. The heat pump penetration is therefore

$$\% \text{ penetration of heat pumps} = (n/24) \times 100$$

where 'n' is the number of heat pumps 'on'.

It was found that, if the coincidence factor (the ratio, expressed as a numerical value or as a percentage, of the simultaneous maximum demand of a group of electrical appliances or consumers within a specified period, to the sum of their individual maximum demands within the same period) of existing loads on the network is 0.7, the network, under a worst-case scenario, can accommodate additional load equivalent to a 20% penetration of heat pumps. However, it is worth noting that the low voltage (LV) substation transformers are the only elements to be overloaded as heat pump load increases beyond this level. No other elements are even close to their rated values. For example, for a 50% penetration of heat pumps, the highest loading of a line is 32%. The LV substation transformer bottleneck has also been highlighted in [11] in relation to electric vehicle charging. It should be noted that the transformer overloading can be avoided, to a certain extent,

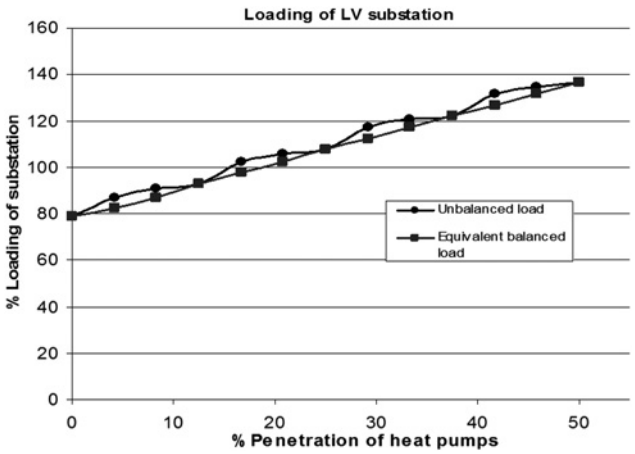

Fig. 5 *Loading of LV substations with increasing penetration of heat pumps*

doi: 10.1049/iet-gtd.2014.0056

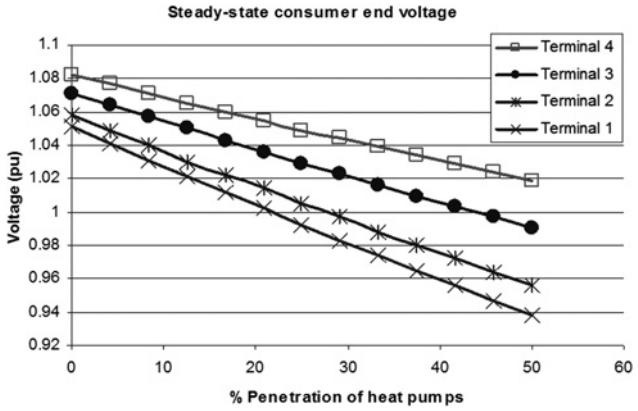

Fig. 6 *Variation in steady-state voltage with heat pump penetration*

by deferring heat pump load at peak times. The implications of this for consumer comfort will be considered later. Fig. 5 shows the loading profile of the LV substation involving the two-winding transformer (9) from the network diagram. As this substation is modelled in detail, it represents exact loads from unbalanced phases. The equivalent balanced load curve is obtained for the lumped LV substations (the lumped loads LL1–LL7). Equivalent balanced loads increase the system loading linearly, whereas unbalanced loads increase it more markedly when a load is added on a single phase in addition to a balanced load. The existing UKGDN loads are three phases represented by LT1, LT2, LT3 and LT4 in the network diagram and represent the equivalent three-phase load of 24 customers.

The steady-state voltage at the consumer terminals is an important consideration. The voltage at the four clusters is well within limits (0.95 pu) up to 37% penetration, as shown in Fig. 6.

Beyond 37% penetration, the steady-state voltage at Terminal 1, the most remote, drops below 0.95 pu.

5.2 Transient voltage and impact of single-phase switching on other phases

The transient voltage during the switching process has been recorded in a sequence by increasing heat pump load in steps. The results are summarised in Fig. 7.

The nine graphs show both the effect of unbalance and an increasing penetration of heat pump load. The first row of graphs show the switching transients when one heat pump is switched in phase A only (1A + 0B + 0C), then phases A and B (1A + 1B + 0C) and finally in all three phases simultaneously (1A + 1B + 1C). In the second row, the sequence is repeated with an extra heat pump in all three phases. The third row depicts the transients when there is a further heat pump in all three phases. The heat pump penetration ranges from 1 out of 24 (4.2%) at the top left of Fig. 7 to 9 out of 24 (37.5%) at the bottom right. The first and second columns depict unbalanced heat pump load, whereas the third column shows balanced load. The graphs show the variations in all three-phase voltages, A, B and C.

It may be seen from Fig. 7(i) that, with one heat pump in phase A only, the voltage drops to 86% on phase A whereas the voltages on phases B and C rise to 115 and 110%, respectively, during starting. When two heat pumps

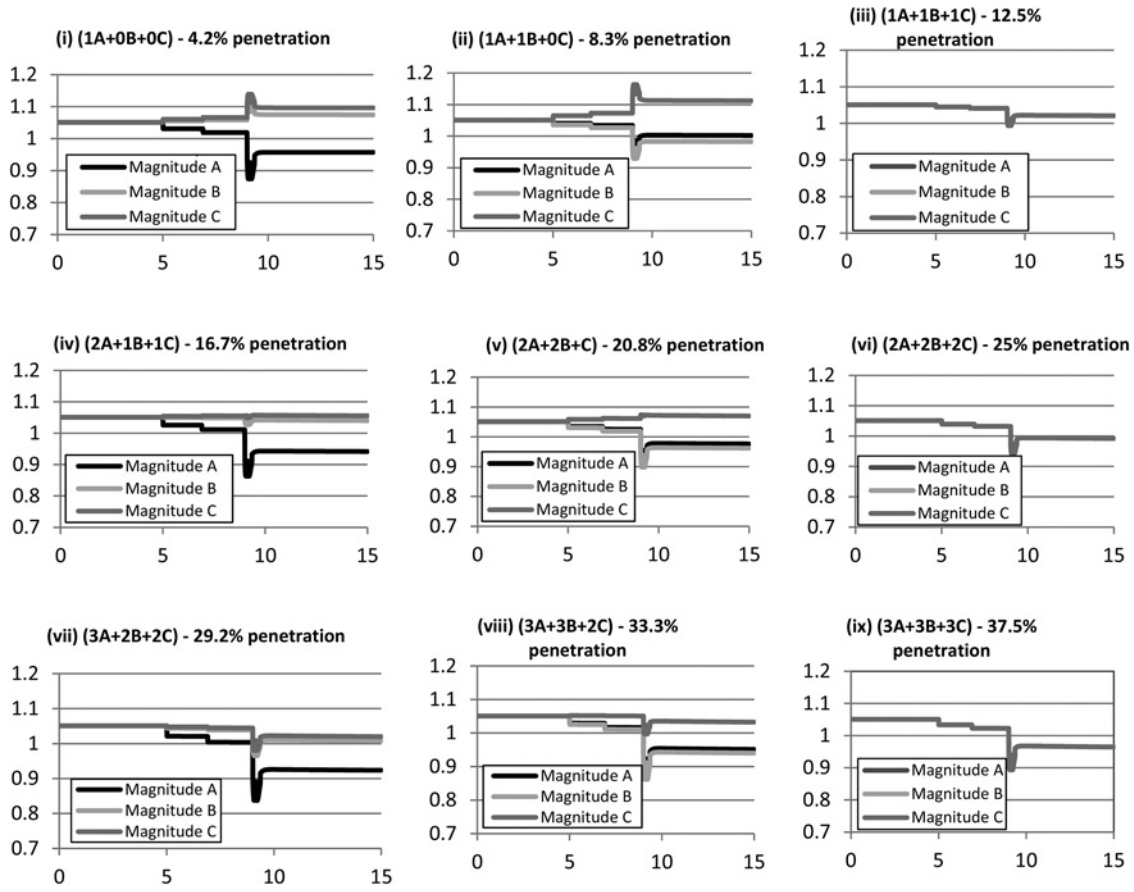

Fig. 7 *Transient voltages during switching of heat pumps – pu voltage against time in seconds*

doi: 10.1049/iet-gtd.2014.0056

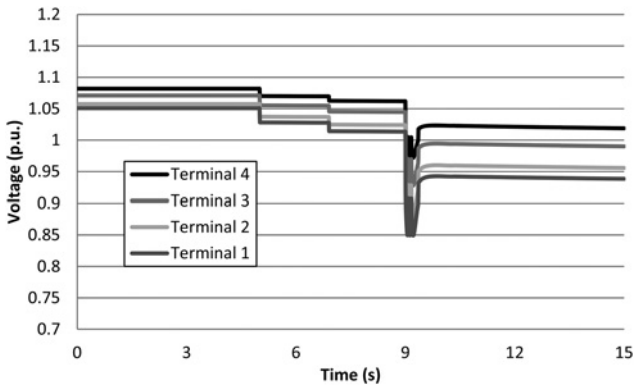

Fig. 8 *Voltage variations when heat pumps are switched on simultaneously*

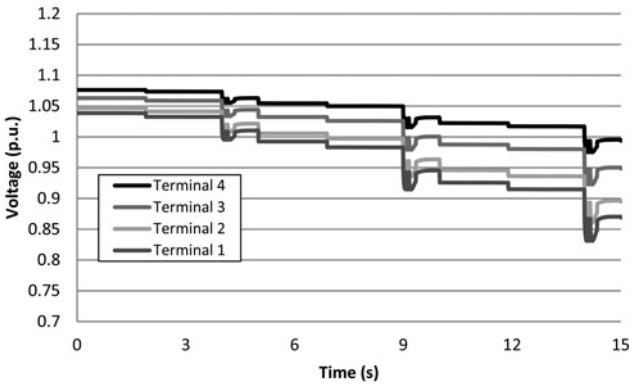

Fig. 9 *Variation in system voltage when heat pumps are switched on simultaneously one phase at a time*

were switched on together in phases A and B, as shown in Fig. 7(ii), the voltage drops to 95 and 93%, respectively, on these phases whereas the voltage rises on phase C to 117%. With three heat pumps, one in each phase such that the load is balanced, the voltage transient was the same for all three phases and is much less compared with the previous cases of unbalanced loading.

When the number of heat pumps is increased but the loading is unbalanced, such as in Figs. 7(iv) and (v), the voltage transients on adjacent phases are less pronounced than before. This is because heat pumps installed on adjacent phases lead to voltage drops that tend to balance the voltage rises at the switching instant. The maximum voltage drop, to 83% in phase A, occurs in Fig. 7(vii), where the heat pump penetration is 29.2%. When the penetration is higher, at 37.5%, but with balanced loading, the transient voltages in all three phases fall to 89% – see Fig. 7(ix).

The voltages recover to within 95%, or very close, except for the case shown in Fig. 7(vii) with an unbalanced penetration of 29.2%. In contrast, the higher but balanced concentration of 37.5% depicted in Fig. 7(ix) results in less severe transients and satisfactory recovery voltages. Hence, it may be concluded that a heat pump penetration of 37.5% can be accommodated, provided the load is balanced, with simultaneous switching across the three phases.

5.3 Switching sequences

The 'worst case' might be expected to occur when all heat pump load is switched simultaneously. That is the scenario depicted in Fig. 8 for a 50% penetration. The load is switched on at 5 s. The effect of the soft-starter is evident from the voltage steps 2 and 4 s after switch-on. The voltages in all phases reach a minimum of 85% of nominal at 9 s. However, the voltages have recovered to over 94% by 10 s.

An alternative procedure might be to switch-on supply to all heat pump loads in phase A, then phase B and finally phase C. The transient voltages resulting from this sequence are shown in Fig. 9, where the A phase load is energised at 0 s, the B phase at 5 s and the C phase at 10 s. It may be seen that the lowest voltage during the transient is 83%, and the lowest recovery voltage is 87%. It may therefore be concluded that simultaneous switching across the phases is to be preferred to staggered switching of the phases. This conclusion is consistent with the effect of switching described in Section 5.2 above and illustrated in Fig. 7, where the balanced switching of all three-phase loads has less impact on voltage than unbalanced switching of a smaller load.

Fig. 10 shows the voltage variation on consumer terminals (three-phase) when a random delay of 0–15 s was applied to a 50% heat pump penetration. There are interesting voltage

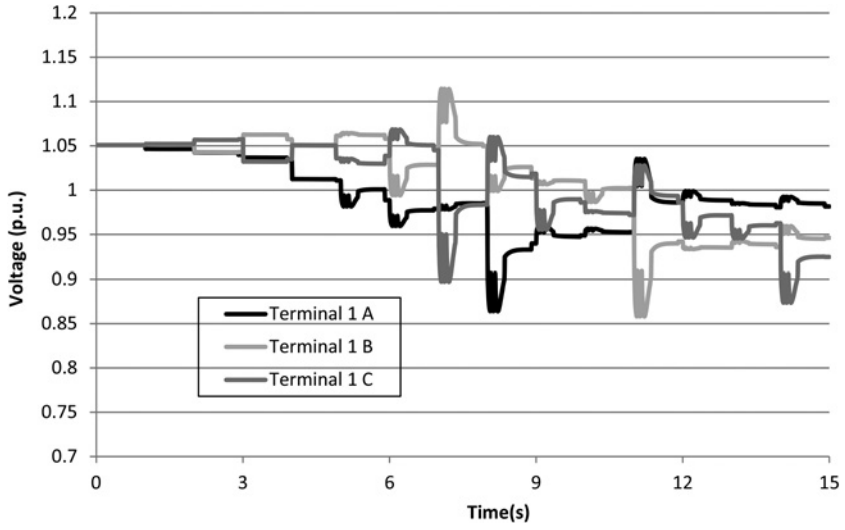

Fig. 10 *Variation in single-phase voltages when heat pumps are switched on with a random delay of 0–15 s*

doi: 10.1049/iet-gtd.2014.0056

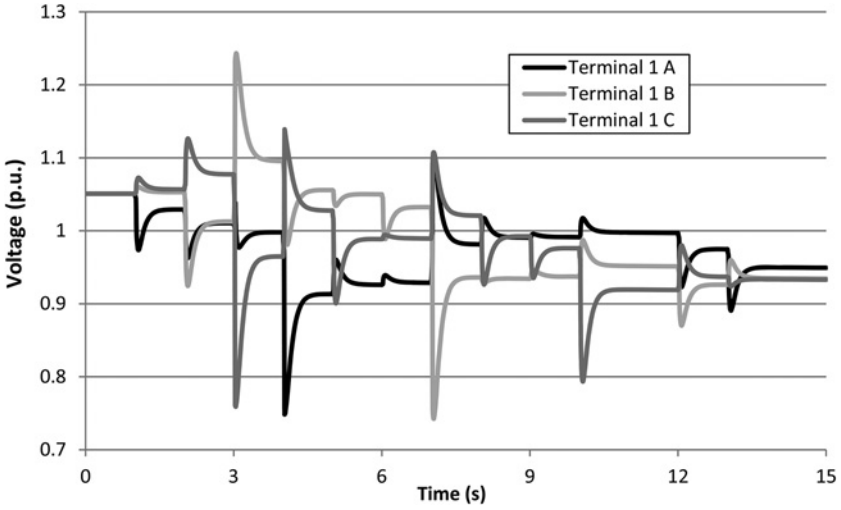

Fig. 11 *Variation in system voltage for heat pumps without soft-starter, started randomly between time 0 and 15 s*

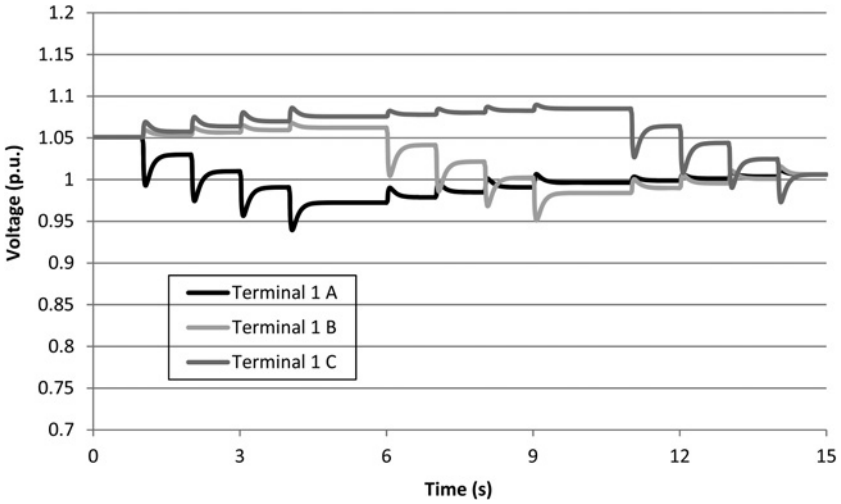

Fig. 12 *Heat pumps without soft-starter started in a sequence of increasing heat pumps on one phase at a time*

variations on single-phase terminals with the random switching scenario.

6 Heat pump compressor motor without soft-starter

There are still some cases where heat pumps are supplied with compressor motors without soft-starters. Some examples are given in realistic analysis of the impact on low-voltage networks by National Energy Action [12]. The heat pump model was updated to replicate the starting characteristics of a single-phase induction motor without soft-starter. For this purpose, the model developed in Section 3 is modified in such a way that the input variables are all similar, eliminating the staged start-up and reflecting only a higher peak current.

The equations used for simulating the heat pump without the soft-starter are as follows (see (7)).

The remaining part of the model remains the same. This time no time delay is required to limit the peak current. For a 10 kW (heat output) heat pump, the starting current of the compressor is 45–50 A without a soft-starter.

Fig. 11 shows the system voltage disturbances for random switching of a 50% penetration of heat pumps without soft-starters. It can be noted that voltage drops to <80% on many occasions.

7 Changes in network modelling to see the impact of single heat pump switched on each phase

To see the impact of single heat pump switching on different phases, the modelling has been modified such that the lumped loads do not show similar changes in switching. Only 'Terminal 1' is having additional heat pumps installed as shown in the network diagram (Fig. 4).

$$P = \begin{cases} 0, & \text{if } t \le t_s \\ x_p \times \left(1 + 6 \times e^{(-1\times(t-t_s)/T)} - 6 \times e^{(-4\times(t-t_s)/T)}\right), & \text{if } t > t_s \end{cases} \quad (7)$$

doi: 10.1049/iet-gtd.2014.0056

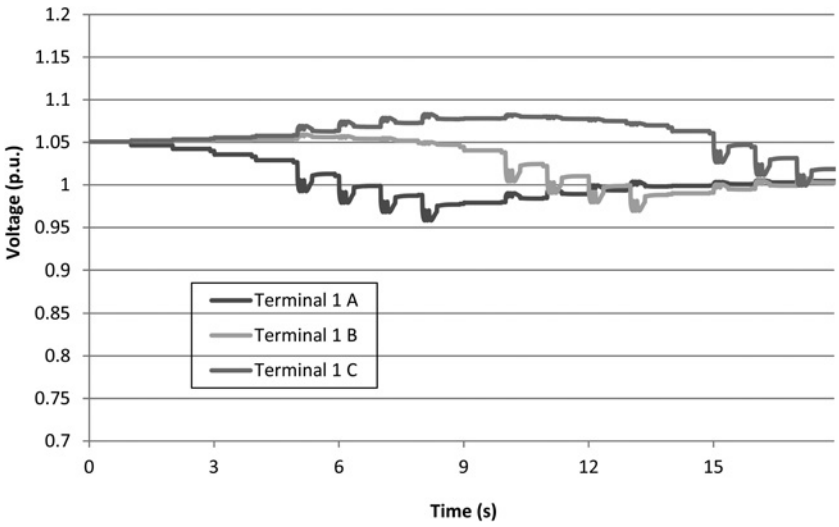

Fig. 13 *Heat pumps with soft-starter started in sequence*

The lumped loads no longer have any additional heat pump loads installed.

The switching of heat pumps on all three phases of Terminal 1 is considered in a sequence of top to bottom (LTA 01–LTA 04, then LTB 01–LTB 04 and finally LTC 01–LTC 04). This will represent a maximum of 50% penetration. Fig 12 shows the change in voltage in all three phases when heat pumps without soft-starters were switched on in the above sequence. Fig. 13 shows a similar scenario with soft-starters.

8 Heat pump load diversity

The simulation results presented above, especially those for unbalanced loading, tend to exaggerate the switching transients and steady-state voltage deviations. For example, the transients shown in Fig. 7 assume that all heat pumps are switched on simultaneously, which is the worst case that can be envisaged. In practice, switching will be random within and between phases, attenuating the variations shown in the simulations. Overall heat pump load will be determined by ambient temperature. At a given temperature, heat pumps being switched on one at a time across the network will be balanced by others being switched off. Thus, there will be many small transients of the type shown in Fig. 7. However, the voltage deviations will depend on the number of heat pumps on load at a given time. Only in very cold weather would the overall loading approach the penetrations modelled in the simulations. Thus, for the maximum penetration considered of 37.5%, the actual voltage deviation would be less than the simulated value shown in Fig. 7(ix). Given normal load diversity, a heat load penetration of 50% could probably be achieved for the generic network before transient or steady-state limits are breached.

However, there is an important caveat. Heat pumps are likely to be subject to a tariff that offers cheaper electricity and traditionally this would have been provided winter evening peaks, typically 4.00–7.00 p.m., are avoided. Owing to cooling during these hours, a peak-avoidance tariff would result in a loss of diversity, with coherent switch-on of most heat pumps at the end of the peak period. The conditions would then exist for the extreme scenarios examined in the simulations above. In future, however, it is envisaged that tariffs for heat pump and other schedulable load will probably be real-time based and reflect both available generation (and in particular renewable generation) and also distribution system available capacity to deal with such load. Real-time tariffs coupled with a block switching approach similar to that previously adopted for space and water heating [13] is thought to offer a practical solution for the control or incentivisation of heat pump load at appropriate times.

9 Conclusion

This paper discusses the operation of the low-voltage network after adding heat pumps to the existing system.

A special-purpose model of a single-phase induction motor compressor drive was developed. Taking into consideration a high penetration of such devices, the operation of a generic low-voltage network has been analysed and presented. The analysis has shown that if 20% of customers install heat pumps, the grid under investigation will not be overloaded. However, even with soft-starters, the transient voltage drops exceed statutory limits, as in many cases the voltage is observed to fall below 90% of nominal. It was found that the transient disturbances were minimised by switching the heat pumps on all phases simultaneously.

The paper also examined the effect of heat pump load without soft-starters. Transient effects were more pronounced, showing that soft-starters are required to maximise heat pump deployment.

10 Acknowledgment

This work was supported by a Charles Parsons Energy Research Award, which is funded by Science Foundation Ireland (SFI), award (06/CP/E002).

11 References

1 MacKay, D.J.C.: 'Sustainable energy – without the hot air' (UIT Cambridge Ltd, 2009)

2 Saner, D., Juraske, R., Kübert, M., Blum, P., Hellweg, S., Bayer, P.: 'Is it only CO_2 that matters? A life cycle perspective on shallow geothermal systems', *Renew. Sustain. Energy Rev.*, 2010, **14**, (7), pp. 1798–1818

doi: 10.1049/iet-gtd.2014.0056

3 Arteconi, A., Hewitt, N.J., Polonara, F.: 'Domestic demand-side management (DSM): role of heat pumps and thermal energy storage (TES) systems', *Appl. Therm. Energy*, 2013, **51**, pp. 155–165
4 Gers, J.M.: 'Distribution system analysis and automation'. IET, 2013
5 Ingram, S., Probert, S.: 'The impact of small-scale embedded generation on the operating parameters of distribution networks'. P B Power, Department of Trade and Industry (DTI), 2003
6 Cipcigan, L.M., Taylor, P.C., Lyons, P.: 'A dynamic virtual power station model comprising small-scale energy zones', *Int. J. Renew. Energy Technol.*, 2009, **1**, (2), pp. 173–191
7 Boemer, J.C., Gibescu, M., Kling, W.L.: 'Dynamic models for transient stability analysis of transmission and distribution systems with distributed generation: an overview'. Proc. IEEE PowerTech, Bucharest, 2009, pp. 1–8
8 Price, W.W., Taylor, C.W., Rogers, G.J.: 'Standard load models for power flow and dynamic performance simulation', *IEEE Trans. Power Syst.*, 1995, **10**, (3), pp. 1302–1313
9 Hughes, E.: 'Electrical and electronic technology' (Pearson, 2008, 10th edn.)
10 Akmal, M., Fox, B., Morrow, D.J., Littler, T.: 'Impact of high penetration of heat pump load on distribution networks'. IEEE PowerTech, Trondheim, 2011
11 Fairley, P.: 'Speed bumps ahead for electric-vehicle charging'. IEEE Spectrum, January 2010, pp. 13–14
12 Lynch, D.: 'Air-source heat pumps – assessing the implications for the electrical distribution system'. Department of Energy and Climate Change, UK, 2010
13 McCartney, A.I.: 'Load management using radio teleswitches within NIE', *IEE Power Eng. J.*, 1993, **7**, (4), pp. 163–169

doi: 10.1049/iet-gtd.2014.0056